Rev.Adv.Mater.Sci. 15(2007) 105-110

FIBER TEXTURE DEPENDENCE OF THE ANISOTROPIC RESIDUAL STRESS STATE INDUCED BY LATTICE DISTORTION IN ARC-EVAPORATED Ti-Al-N THIN FILMS

C.V. Falub[1,2], A. Karimi[1], F. Fontaine[3] and W. Kalss[3]

[1] Institut de Physique de la Matière Complexe (IPMC), École Polytechnique Fédérale de Lausanne (EPFL), CH-1015, Lausanne, Switzerland

[2] present address: Nanoscale Materials Science, Swiss Federal Institute for Material Testing and Research (EPMA), Ueberlandstrasse, 129, CH-8600 Debendorf, Switzerland

[2] Balzers AG, Iramali 18, FL-9496 Balzers, Principality of Liechtenstein

Received: January 22, 2007

Abstract. We present recent XRD results on the residual stress state and fiber texture of Ti-Al-N thin films grown on WC-Co and tool steel substrates using arc-evaporation method. Reciprocal space maps around 002 TiAlN reflection revealed a subtle oscillatory behavior of the lattice spacing versus $\sin^2\psi$ curves, which is dependent on the magnitude of the stresses in the films. Pole figure XRD measurements have demonstrated that the fiber texture of the films is (311) and that their crystalline structure deviates from the ideal B1-fcc structure of TiN. Consequently, using the general elastic theory for textured materials, the anisotropic behavior of the 002 TiAlN reflection was attributed to the distorted lattice of the (311) oriented films.

1. INTRODUCTION

The analysis of residual stress state is of great technological importance because stresses can improve or degrade the mechanical properties of thin films [1]. For example, the compressive residual stress is desirable to some extent retarding crack propagation and improving the fracture toughness of hard coating. However, exessive compressive stress may promote poor adhesion of the film to the substrate or cohesive fracture in the film [2]. Additionally, preferred orientation of crystallites or fibre texture, i.e. a crystallographic axis aligned along the global growth direction, has a profound effect on anisotropy of elastic properties and thermal expansion that are essential for the mechanical stability of films [3].

In this paper, we study the stress state and fiber texture of cathode arc evaporated TiAlN thin films used in the hard coating industry.

2. EXPERIMENTAL

TiAlN coating studied in this work were deposited by cathode arc evaporation process on various polished substrates: tungsten carbide (WC-Co) and two different tool steel substrates, e.g. a soft tool steel denoted as TS (~ 6.6 GPa) and a hard high-speed steel denoted as HSS (~ 14.5 GPa). Details of the deposition system (an industrial unit type RCS from Balzers) and deposition conditions can be found elsewhere [4,5]. The morphology and structure of the coatings were investigated by scanning electron microscopy (SEM) using a Philips FEG-XL 30 microscope and the chemical composition was determined with energy-dispersive X-ray spectroscopy (EDS). The crystallographic phases, residual stress and fiber texture of the coatings were characterized by X-ray diffraction measurements (Cu-K_α radiation) using a computer-controlled laboratory diffractometer (Seifert XRD

Corresponding author: C.V. Falub, e-mail: claudiu.falub@empa.ch

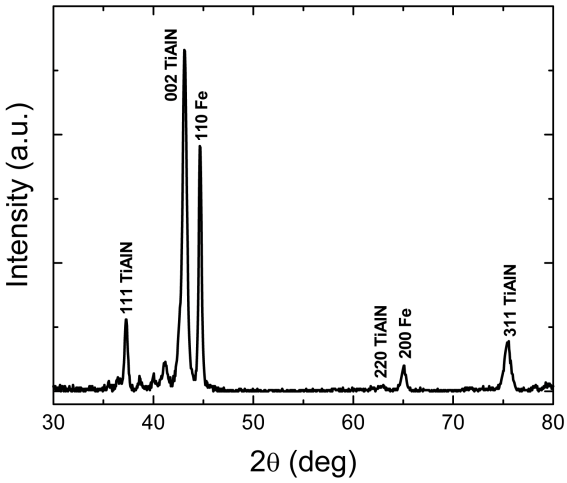

Fig. 1. XRD pattern in Bragg-Brentano configuration for TiAlN coating deposited on TS.

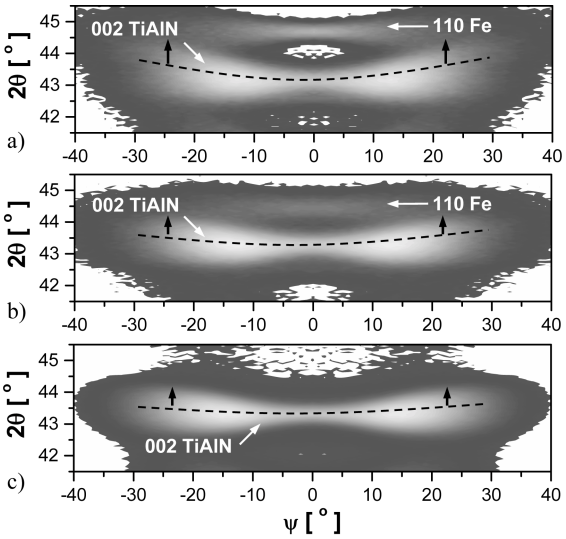

Fig. 2. XRD reciprocal space maps measured around the 002 TiAlN reflection of TiAlN coating deposited on TS (a), HSS (b) and WC-Co (c). Dashed curves indicate the shift of the maximum in the 002 TiAlN reflection and arrows show the shift of this maximum when the sample is tilted.

3003 PTS-HR) with a four-circle goniometer. To determine residual stresses, glancing angle (θ = 4º) X-ray diffraction (GAXRD) and reciprocal space map (RSM) analysis around 002 TiAlN were performed. Fiber texture was determined from XRD measurements in Bragg-Brentano (BBXRD) θ - 2θ configuration and, more systematically, by analyzing the pole figures (PF) measured around 111, 002, 220 and 311 reflections.

3. RESULTS AND DISCUSSION

Cross-sectional SEM performed on the fractured samples showed a dense structure with a pronounced columnar microstructure and EDS measurements revealed that the Al content in the TiAlN coatings is ~ 44% [5]. XRD measurements showed that, apparently, the films exhibit (002) textures, as shown for example in Fig. 1 for the TiAlN coating deposited on TS. The residual stresses were determined by monitoring the shift of the maximum position of the 002 TiAlN Bragg reflection at different tilt angles (ψ). Fig. 2 presents the RSM's measured around the 002 TiAlN Bragg reflection of TiAlN coatings deposited on TS, HSS and WC-Co substrates. The shift of the 002 TiAlN maximum towards larger angles (i.e. smaller lattice parameter) suggests that the coatings are compressively stressed. In addition, one observes that the shift of 002 TiAlN maximum is more pronounced for the coatings deposited on TS than those deposited on HSS and it is even more pronounced than for the coatings deposited on WC-Co. Thus, the compressive residual stress is highest for the coatings deposited on TS and lowest for the coatings deposited on WC-Co.

From the RSM's in Fig. 2 one can obtain the lattice spacing (a_ψ) of the TiAlN coatings deposited on TS, HSS and WC-Co versus the $\sin^2\psi$ (open dots in Fig. 3a). On the same figures the solid dots represent the lattice spacing determined from GAXRD measurements. While in the RSM there is no limitation in the ψ spacing (in our case a 1° step was employed), the limited number of available reflections in the GAXRD pattern (e.g. 111, 200, 220, *etc.*) does not allow an accurate determination of the stress state. On the other hand, the beam defocusing at large tilt angles puts a restriction on the $\sin^2\psi$ range for which the lattice spacing can be determined, while with GAXRD one is not limited in the $\sin^2\psi$ range as long as there are still reflections available in the diffraction pattern. Nevertheless, one observes that there is a good agreement between the lattice spacing values obtained with the two different techniques.

Assuming an equal-biaxial stress state, the residual stress in the coatings can be determined by applying the traditional $\sin^2\psi$ method (i.e. by linear

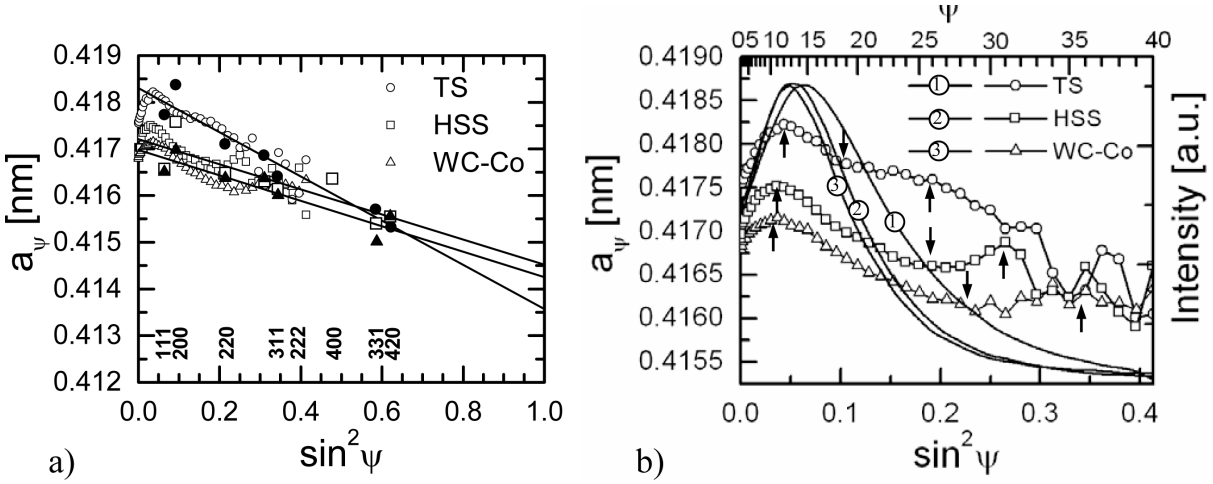

Fig. 3. a) Lattice spacing (a_ψ) versus $\sin^2\psi$ plots for TiAlN coating deposited on TS, HSS and WC-Co. Open dots correspond to data obtained from the 002 RSM's, while solid dots to data obtained from GAXRD; straight lines are the linear fit through the experimental points. b) a_ψ – $\sin^2\psi$ plots represented on a smaller scale. Arrows indicate maxima and minima of the oscillating curves. Labeled lines represent the intensity of the maxima in the 002 TiAlN reflection plotted against the tilt angle (ψ).

fitting the a_ψ vs. $\sin^2\psi$ curves) [1]. Thus, we obtain -4.1, -3.3, and -2.1 GPa for the stress values in the coatings deposited on TS, HSS and WC-Co, respectively. The change in the magnitude of residual stress in the coatings deposited on various substrates can be explained based on the difference in thermal stress contributions induced by the different thermal expansion coefficients of the substrates and this has been detailed elsewhere [5]. However, these results are based on the linear isotropic elasticity, i.e. a linear dependence between a_ψ and $\sin^2\psi$. This method can only be applied for non-textured samples formed of elastically isotropic crystallites, for which there is no direction-dependent grain interaction [1]. In practice, however, polycrystalline materials are formed of elastically anisotropic crystallites for which the presence of direction-dependent grain interaction and/or crystallographic texture is frequently encountered.

A closer inspection of the experimental stress curves reveals that for all samples there is a clear deviation from linearity, i.e. an oscillatory behavior (see Fig. 3b). In the same figure labeled solid lines depict the intensity of the 002 TiAlN maximum versus the tilt angle ψ. With arrows oriented upwards and downwards we indicate the relative maxima and minima of the oscillatory curves.

Deviations from linearity of the stress curves occur because, in general, for an anisotropic elastic material, the stress is a triaxial tensor, σij; $i,j = \{x,y,z\}$, where x, y and z are the coordinate axes of the specimen with z being perpendicular to the surface [6-8]. In the presence of the shear components of the stress tensor perpendicular to the surface, e.g. σ_{xz} and σ_{yz}, an additional term proportional to $\sin 2\psi$ should be considered in the equation that describes the dependence between the lattice spacing a_ψ and the tilt angle ψ[1]. One should point out that the shear stresses σ_{xz} and σ_{yz} can only exist as gradients since, by definition, these components must vanish at the surface of the samples. Hence, the trigonometric term $\sin 2\psi$ comes because the measured stress is an average value over the penetration depth of the X-rays, which decreases when the tilt angle increases. Similarly, if any of the normal stress components (σ_{ii}) or the shear stress (σ_{xy}) exhibits gradients with depth, the stress curves will deviate from linearity with a trigonometric $\sin 2\psi$ term. This term would cause a 'ψ splitting' of the lattice spacing versus $\sin^2\psi$ curves for $\psi < 0$ and $\psi > 0$. Indeed, we observed small differences between stress curves at $\psi < 0$ and $\psi < 0$ (not shown here), but the oscillations observed in Fig. 3d cannot be attributed to

1 The shear stress σ_{xy} component gives a contribution that is proportional to $\sin^2\psi$.

the shear stresses, since the additional trigonometric term sin2ψ has only a maximum (minimum) at ψ=45° (-45°). Moreover, we observe a striking feature of these oscillations and that is that their period is apparently dependent on the substrate on which the coating was deposited. Thus, the smallest period is observed for the coating deposited on TS, while the highest one for the coating deposited on WC-Co. Since these are also the coatings that in average have the highest and lowest total residual stress, as measured by using the 'sin^{2}ψ method', the oscillations of the stress curves seem to be related to the magnitude of the stress. However, since the thermal stress is biaxial, the change of the oscillations period should only be related to the intrinsic stress, or to other reasons that we pointed out during our discussion.

The variation of normal and shear stresses with depth is not the only possible explanation of the perturbation from linearity of the stress curves. A concentration gradient with depth combined with the variable penetration depth during the stress measurements may also cause such effect. However, accurate depth dependent composition measurements are necessary to determine whether such gradients are present. Nevertheless, earlier TEM investigations of similar samples showed a nanolayered structure with a concentration that seems to be modulated over the whole thickness [4].

Moreover, due to the variable incidence angle of the incoming ions during the deposition the difference in sputtering yield between aligned and misaligned grains can play an important role for the intrinsic stress caused by atomic peening. It can be argued that for the misaligned grains the atomic peening is lower than for the aligned grains, since a higher amount of resputtered particles will occur for the first category of grains. These effects can also play an important role in the formation of the coating fiber texture.

Another possible explanation for the oscillations of the stress curves seen in Fig. 3 is the fiber texture of the coating. For a textured material the equation relating the lattice spacing $a_{\psi\varphi}$ with the tilt and azimuth angles (e.g. ψ and φ) takes into account anisotropic averages of the x-ray elastic constants over the preferred orientation and has a very complex oscillatory dependence [6]. However, it was shown that for cubic materials residual stress measurements on the (h00) and (hh0) planes should show the same behavior as for isotropic materials, and thus a linear dependence on sin^{2}ψ [6]. Hence,

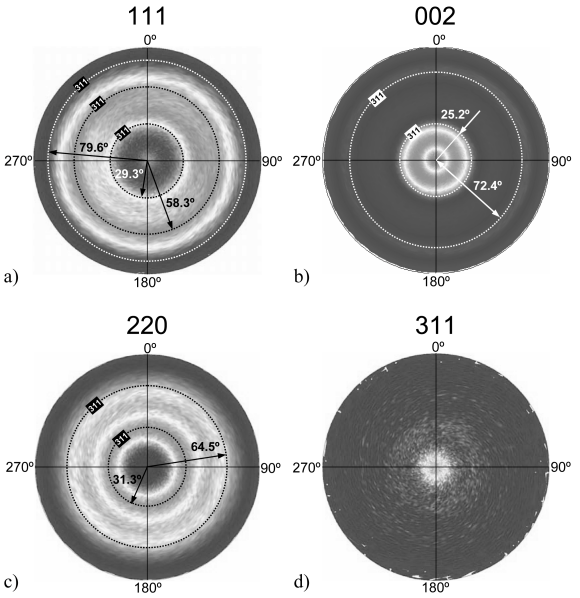

Fig. 4. XRD pole figures for TiAlN coating deposited on tool steel measured around: a) 111; b) 002; c) 220; d) 311 Bragg reflections showed in Fig. 1. Dotted lines indicate the expected ring positions if no distortion is present in the structures.

by assuming that TiAlN has a B1-fcc structure no anisotropy in the sin^{2}ψ dependence should be observed in the 200 TiAlN reflection used to determine the stress state. However, one could imagine that a high fraction of Al alloying may distort the B1-fcc structure of TiN. We will demonstrate that this is true, but let us consider again the Fig. 3b.

As mentioned before, besides the stress a_ψ vs. sin^{2}ψ curves we plotted on the same graph the maximum intensity of the 002 TiAlN reflection against the tilt angle (ψ). This plot is in fact similar to a cross section through a PF and thus is related to the fiber texture with the only difference that the 2θ position changes due to the residual stress state. We observe that the maximum of these 'texture plots' is at about 12-15° and it shifts with the magnitude of the stress in the same direction as the first maximum of the oscillating stress curve. Moreover, it is interesting that the FWHM of these plots seems also to be related to the magnitude of the stress. Thus, the texture plot for the coating deposited on TS has the broadest shape and it corresponds to the highest average residual stress. Previously, we have reported tilted textures in arc evaporated Ti-Al-N films and that for the same coating deposited on the same substrate there is an

Table 1. Polar angles of the texture components obtained by decomposing the cross sections through 111, 200 and 220 pole figures at ϕ = 0º. The values in brackets represent the polar angles for (311) oriented B1-fcc crystal.

ψ [º]			
111	002	220	311
38º (29.50º)	14.5º (25.23º)	32.1º (31.28º)	0º (0º)
56º (58.51º)	77º (72.45º)	61.3º (64.76º)	- (35.10º)
71º (79.98º)		90º	- (50.48º)
			- (62.96º)
			- (84.78º)

interdependence between the tilt of the texture and the residual stress in the coating [5].

Let us discuss now the results of the pole figure XRD measurements. Fig. 4 presents the PF's measured around 111 (2θ = 37.3°), 002 (2θ = 43.1°), 220 (2θ = 62.9°) and 311(2θ = 75.4°) Bragg reflections of TiAlN film deposited on TS. The PF can be decomposed into several rings with radii given in Table 1. It is clear that the fiber texture of the sample is (311) and not (200) as predicted by BBXRD measurements. This apparent contradiction is related to the lower scattering efficiency of (311) planes and lower fraction of X-rays scattered by the film due to the higher penetration depth at 2θ = 75.4°. Moreover, the fiber texture of the coating deposited on HSS and WC-Co was also (311). The explanation of the various rings in the PF's is as follows. A (311) oriented B1-fcc cubic single crystal will contribute to the 111 PF with three reflections at 29.5° (e.g. 311, 113 and 131), six reflections at 58.51° (e.g. $3\bar{1}1$, $31\bar{1}$, $13\bar{1}$, $\bar{1}31$, $\bar{1}13$ and $1\bar{1}3$) and three reflections at 79.98° (e.g. $3\bar{1}\bar{1}$, $\bar{1}\bar{1}3$ and $\bar{1}3\bar{1}$). For a (311) textured polycrystalline cubic material, however, three rings at 29.5°, 58.51° and 79.98°, respectively, should be obtained. The two rings in the 002 PF are due to the reflections corresponding to the four 1st order and twelve 2nd order <311> planes that make angles of 25.23° and 72.45° with the (001) plane. In the same way, one can explain the features in the 220 PF.

Similar to the small shifts of the maximum of texture plots in Fig. 2, we observed substrate dependent shifts of the rings in the 111 and 002 PF's of the order of a few degrees. Since the (311) fiber texture remains unchanged, these substrate dependent slight modifications of the 111 and 002 PF's already suggest that apparently there is some lattice distortion present in the structures. Stronger arguments for the lattice distortion can be obtained if one compares the rings radii in the 111 and 002 PF's with the theoretical values corresponding to a (311) textured cubic material (see Table 1). The most evident difference is observed in the 002 PF, where the first ring is shifted by ~ 10.7° towards lower polar angles, while the second ring is shifted by ~ 4.6° towards higher polar angles. For 111 PF deviations from the expected radii are also observed, but at least for the most intense ring, i.e. at 56.3°, the difference is not so significant. For the other two rings, the displacements seem to be more pronounced with respect to the theoretical values, but since the intensity of these are weak, it is more difficult to estimate their exact position. Nevertheless using the positions of the first and second ring in the 002 PF, one can give an estimate of the distortion in the sample as follows. Assuming a cubic to orthorhombic transformation ($a \neq b \neq c$, $\alpha = \beta = \gamma = 90°$), and defining the parameters $x = c/a$, $y = c/b$ and ψ_1, ψ_2 the radii of the first and second ring in the 002 PF, one obtains the following expressions $x = 2/\sqrt{2}\,(1/\cos^2\psi_2 - (2/3\tan\psi_1)^2 - 1)^{1/2}$ and $y = x/((2x/3\tan\psi_1)^2-1)^{1/2}$. In the case of zero distortion (i.e. ψ_1= 25.23°, ψ_2= 72.45°) one obtains $x = y$ =1, while for the experimental radii ψ_1= 15° and ψ_2= 77° the values x = 0.79 and y = 0.47 are obtained. Thus, an average lattice unit with $a = 1.27c$ and $b = 2.13c$ is obtained. Using the x and y values found we obtain the following angles between the <311> family of planes and the (111) plane: 25.5°, 37.0°, 41.7°, 44.4°, 52.5°, 58.7°, 59.6°, 66.3°, 68.1°, 72.1°, 79.4°, and 83.6°. One could say that we do not observe so many rings in the 111 PF, but one

could also say that the broad features in the 111 PF are difficult to decompose in several components. However, one observes that the found angles could be grouped into three groups, each one formed of four angles, the first one ~ 40°, the second one ~ 60°, and the third one ~ 75°. Thus, if one averages the angles in each group one obtains 37.1°, 56.9°, and 73.9°, which correspond well with the values 38°, 56°, and 71°° that were found by decomposing the cross section through the 111 PF in three components. In the same way, one can estimate the rings radii in the 220 PF at 43°, 72.9°, and 85.3°. However, these last values are very different with respect to those obtained by decomposing the cross section through the 220 PF, which suggests that our assumption of having a cubic to orthorhombic transformation is not correct and that the lattice distortion is in reality more complex. Another argument in favor of a more complex transformation of the B1-fcc structure of TiN by Al alloying is the fact that using the orthorhombic structure assumption in interpreting the pole figure measurements one obtains an average lattice unit with $a = 1.27c$ and $b = 2.13c$ which seems to be unrealistic. Nevertheless, we have used the orthorhombic structure as a simple model that gave the possibility to analytically solve the information gathered in the pole figure and to show the presence of lattice distortion. In general, a triclinic lattice structure plus additional twisting should be taken into account. By allowing a certain freedom to the α, β and γ around 90°, one may achieve an average lattice unit with $a \neq b \neq c$ that is not too far from a cube, and that can explain better the deviations of the rings in the pole figure experiments. Therefore, a more elaborate study of the texture related lattice distortion in thin films will be published elsewhere.

4. CONCLUSIONS

We have presented an extensive XRD study of the stress-state in arc evaporated TiAlN thin films deposited on tungsten carbide substrates and two different tool steels (e.g. soft and hard). The highest value of the total residual stress was found for the coating deposited on soft tool steel, while the lowest one for the coating deposited on tungsten carbide. This dependence on the nature of the substrate was explained by the difference in thermal residual stress induced by the linear thermal expansion coefficients of the substrates. XRD reciprocal space maps around 002 TiAlN reflection revealed subtle oscillatory behaviors of the lattice spacing versus $\sin^2\psi$ curves, which is dependent on the magnitude of the stresses in the films and various possible responsible mechanisms have been discussed. Pole figure XRD measurements have demonstrated that the fiber texture of the films is (311) and that their crystalline structure deviates from the ideal B1-fcc structure of TiN. Consequently, using the general elastic theory for textured materials, the anisotropic behavior of the 002 TiAlN reflection was attributed to the distorted lattice of the (311) oriented films.

ACKNOWLEDGEMENTS

This work was sponsored by the Swiss Commission for Technology and Innovation (CTI) under Contract No. 69362.

REFERENCES

[1] I.C. Noyan and J.B. Cohen, *Residual Stress. Measurement by Diffraction and Interpretation* (Springer, New York, 1987).
[2] A.E. Santana, A. Karimi, V.H. Derflinger and A. Schütze // *Tribol. Lett.* **17** (2004) 689.
[3] H.R. Wenk and P. van Houte // *Rep. Prog. Phys.* **67** (2004) 1367.
[4] A.E. Santana, A. Karimi, V.H. Derflinger and A. Schütze // *Surf. Coat. Technol.* **177-178** (2004) 334.
[5] C.V. Falub, A. Karimi, M. Ante and W. Kalss // *Surf. Coat. Technology*, in press.
[6] H. Dölle // *J. Appl. Cryst.* **12** (1979) 489.
[7] U. Welzel, J. Ligot, P. Lamparter, A.C. Vermeulen and J. Mittemeijer // *J. Appl. Cryst.* **38** (2005) 1.
[8] K. Helming, R.A. Schwarzer, B. Rauschenbach, S. Geier, B. Leiss, H.R. Wenk, K. Ullemeyer and J. Heinitz // *Z. Metallkunde* **85** (1994) 545.